Journal of Indian Geomorphology
Volume 11, 2023 ● ISSN 2320-0731
Indian Institute of Geomorphologists (IGI)

# Variations in Wave Energy along the Coast between Aksa Beach to Madh Beach, North Konkan, Maharashtra

Deepali Gadkari[1] and Anita Jaiswal[2]
[1]*Department of Geography, University of Mumbai, Maharashtra- 400032*
[2]*SPDT College, J. B Nagar, Andheri (E), Mumbai, Maharashtra 400053*
E-mail: gadhkarideepali72@gmail.com (Corresponding author)

**Abstract:** *Coastal areas are of vital importance from economic and ecological point of view. The most common problems faced by these areas are coastal erosion, siltation and intrusion of marine water inland and in ground water. The basic factors responsible for these problems are the coastal configuration and wave energy patterns which in turn govern the hydrodynamics and the sediment dynamics of the coasts. The present study aims at studying the wave energy dynamics in correlation with the coastal configuration between the Aksa beach in the north and the Madh beach in the south situated on the west coast of India near Mumbai. Wave energy is computed for the selected locations along this stretch by measuring wave parameters such as wavelength, frequency and height. The overall energy condition in the study area reveals a medium energy regime. It is intervened by pockets of high energy and sizably large areas of low energy. High energy pockets are found at the extreme north of the study area, southern ends of the Aksa and Danapani beaches and in the middle of the Madh beach. Strikingly low energy regime is found along Erangal and Bhati beaches situated in the south central part of the study area.*

**Keywords:** *Wave energy, hydrodynamics, sediment dynamics, coastal erosion.*

## Introduction

The coastal zone comprises of diverse and complex environments, shaped by coastal processes, geology and variations in coastline characteristics. Coastal processes relate to physical processes such as waves, tides, currents and winds that act upon and shape the coastline. The coastline is a place where the land and water, come in contact with each other. This contact gives rise to several physical and geomorphic processes which at times can be extremely diverse in nature. The geomorphic processes operating in this region can have both positive and negative impact on the coastal features as well as the life that thrives in these regions (Rahisha *et al.,* 2016). The actions of these forces are responsible for shaping the coastal areas as their collective energy is responsible for onshore and offshore movement of material, which results in deposition and erosion of the coastal areas. The wearing of land or landward displacement of shoreline resulting in coastal erosion or beach erosion is caused by the coastal processes and also by human interventions. The process of coastal erosion continuously changes the shape of the beaches, dunes and coastal cliffs. Detecting such changes plays a crucial role in assessing the sediment dynamics in the areas under consideration. Many researchers (Bioresita and Hayati, 2016; Chenthamilseivan *et al.,*

2014; Di *et al.,* 2003; Nassar *et al.,* 2019; Sreekala *et al.,* 1998) have effectively used remote sensing techniques for monitoring shoreline change.

**Wave energy**

The amount of energy in a wave depends on its height and wavelength as well as the distance over which it breaks. Given equal wavelengths, a wave with greater amplitude will release more energy when it falls back to sea level than a wave of lesser amplitude (Misra and Balaji, 2015; Vicinanza *et al.,* 2011). When the wind passes over the water surface it leads to pressure difference between upper and surface wind, which results in the generation of the wind-waves. When the wind blows over the sea surface, it transfers kinetic energy to the waves; hence these waves carry a lot of power (Tirkey, 2005).

**Study area**

The study area is located along the northwest coast of Mumbai (Fig. 1), extending from 19°08′44.39″ N to 19°10′46.14″ N and 72°46′41.71″ E to 72°48′37.91″ E, covering 6 km of the coastline. The long coastal stretch is characterised by a number of sandy beaches, sand dunes, tidal inlets, mangrove patches and shore platforms. The Aksa beach is a straight beach and is delimited by tidal inlets and shore platform on its southern end. The beach is steeply sloping seaward. The northern limit of the small beach of Danapani is marked by rocky platform and tidal inlet/ estuary with mudflats covered by mangroves.

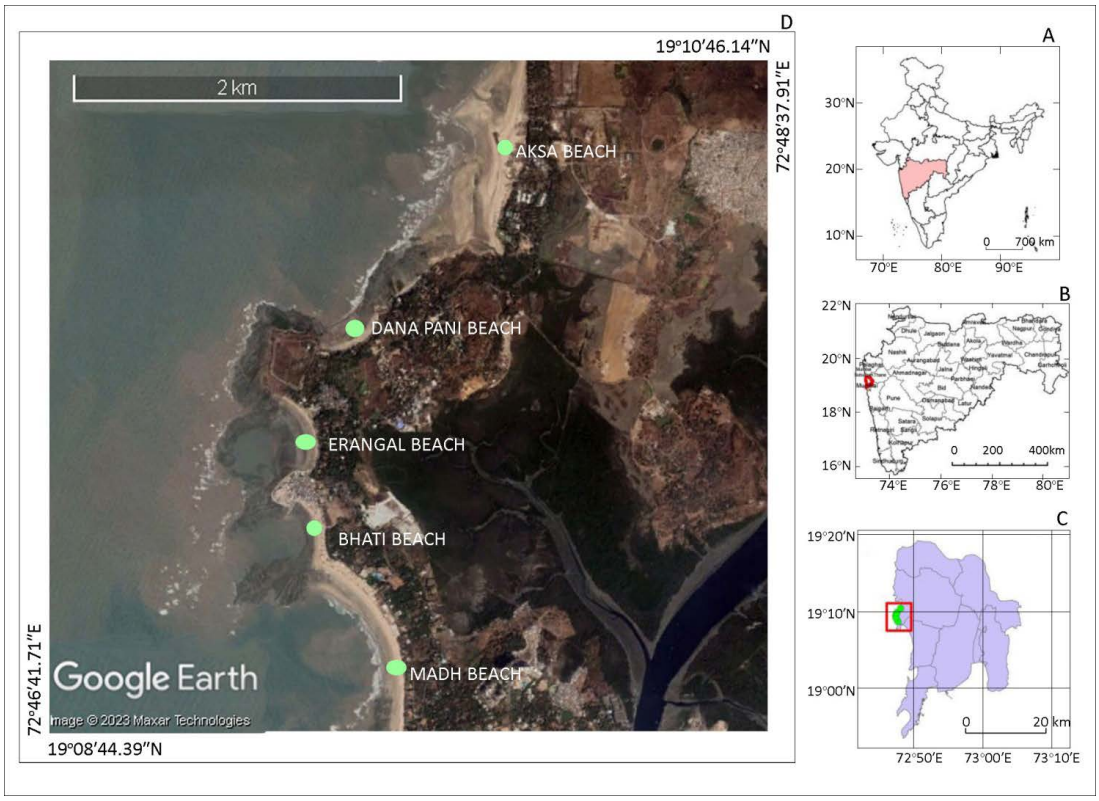


**Figure 1.** Location of the study area: (A) State of Maharashtra within India, (B) Mumbai within Maharashtra, (C) The studied stretch along Mumbai coast, (D) Details of the studied stretch with locations of Aksa, Danapani, Erangal, Bhati and Madh beaches

In the middle of the Erangal beach sand dunes are parallel to the shoreline and the beach is delimited by shore platforms both on its northern and southern ends. A jetty is constructed at the northern end of the Bhati beach. In the backshore area of Madh beach a wall is constructed on the dunes. Cemented platforms are constructed to dry fishes, which occupy the dune area as well as the southern part of the beach. The beach is highly polluted by solid waste littered in the form of plastic bags, bottles and many such non-degradable items.

## Objectives

Wave energy plays an important role in the configuration of coastal areas. High-energy coasts experience erosion at a faster rate than the low-energy coasts which experience more of deposition. In high-energy environment, one can also experience mixing and transportation of sediment within short time spans. The present research work aims to identify the variations in wave energy regimes along the study area and assess the role of wave energy in the development of nearshore sedimentary features.

## Database

The present research is based on wave climate data for calculating the various wave parameters for computation of wave energy at various spots in the study area and temporal images of the coast and nearshore area.

To calculate wave energy, it was necessary to generate data on the wave parameters such as — wave height, wavelength, water depth, wave frequency and wave period. This data was collected in the field at particular study sites. This data was collected at locations in the nearshore zone. Seawater samples and freshwater samples (from the backshore of the study area) were collected to calculate the density of seawater (Table 1).

To observe the temporal changes in the nearshore zone of the study area, google images have been used from year 2004 to 2018. The images of low tide condition were observed where the nearshore features were exposed.

**Table 1.** Data Collection and techniques used

| Parameters | Methods | Total no. of observations | Formula / method | Example |
|---|---|---|---|---|
| Wave height | Computed | 477 | Wave height = height of wave crest – height of wave trough | wave crest (m) = 0.52 wave trough (m) = 0.35<br>Wave height (m) = 0.52–0.35 = 0.17 m |
| Water depth | Measured at 20 locations by putting the staff in water for 15 minutes | Measured at 20 locations for 477 waves | measured with measuring staff | |
| Water density | Computed | Five beaches sample water | Water density = sea water / Tap water | Sea water = 9.829 g<br>Tap water = 9.751g<br>water density = sea water/ tap water = 9.829/ 9.751×1000 = 1007.99 kg $m^{-3}$ |
| Wave energy | Calculated / computed | — | $E = pgH^2/8$<br>Where E = mean wave energy density<br>p = water density<br>g = acceleration by gravity<br>H = wave height | p = 1007.99 kg $m^{-3}$<br>g = 9.8 m/$s^2$<br>H = 0.17m<br>$E = pgH^2/8$<br>$E = 1007.99 \text{ kg m}^{-3} \times 9.8 \times (0.17)^2 / 8$<br>= 3568.53 J $m^{-2}$ |

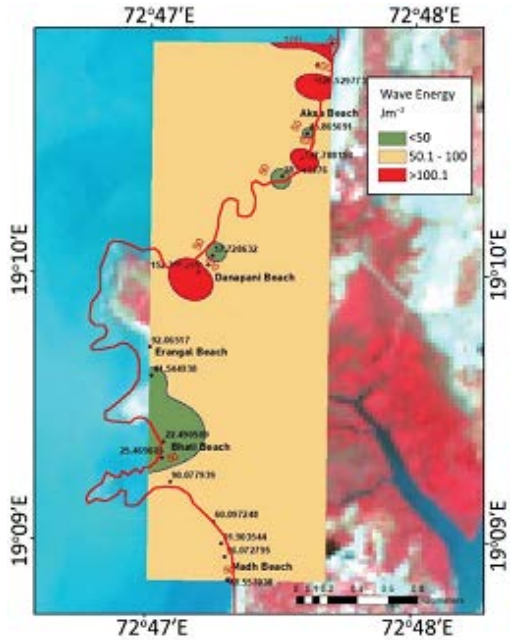


**Figure 2.** Wave energy distribution in the study area

## Methodology

The main components of the methodology are field methods of data collection, processing of field data and computation of wave energy, preparation of vector layers in GIS platform, observing the satellite images, noting the features and finally correlating the wave energy patterns with the features in the nearshore zone. These components are discussed below:

*Generating data on wave parameters*

The shoreline configuration varies from one site to another along the coast due to site-specific hydrodynamic conditions such as wave height, wave direction and wave celerity (Kaliraj, *et al.,* 2014). The wave parameter data was collected at 18 locations in the study area. The geographic coordinates of these locations were recorded through GPS.

To measure the wave height data, the heights of crests and troughs of the approaching waves were noted at each of the 18 locations by holding a levelling staff. At each location, the heights were noted for 15 minutes. Then the difference between the trough and the crest was calculated for each wave and then the values were averaged. This average value has been taken as the wave height for a particular location.

*Calculation of density of seawater*

The density of pure water is 1000 kg $m^{-3}$. Seawater is denser because of the salt in it. The two main factors that influence the density of seawater are temperature and salinity. Temperature and seawater density are inversely related whereas salinity and density are directly related (https://www.windows2universe.org/?page=/earth/Water/density.html).

- Seawater samples were collected from the nearshore area of each of the five selected beaches in the study area. Density was computed for each of these water samples.
- Seawater and freshwater samples were collected and weighed on electronic

balance, to take 10 ml of each type of water sample.

- Density of seawater was computed by applying the following formula and the density values were then used as inputs for computation of wave energy (https://www.youtube.com/watch?v=zHA16IgM5e0).

$$\frac{\textit{Weight of seawater}\ (10\ ml)}{\textit{Weight of fresh water}\ (10\ ml)} \quad \text{..... Equation 1}$$

*Computation of wave energy*

The wave energy for all the five beaches in the study area was calculated using the equation proposed by Dyer (1986).

$$E = \frac{\rho g H^2}{8} \quad \text{..... Equation 2}$$

Where:

E is the mean wave energy ($Jm^{-2}$)

H is wave height (m)

ρ is the sea water density ($gm^{-1}$)

g is the acceleration due to gravity ($ms^{-2}$)

The locations for which energy was computed were plotted on map with wave energy values as attribute data (https://greener4life.com/Wave-Energy-Calculator). Raster layer is generated after interpolating the values by IDW interpolation method done in ArcGis, version 10.3. This raster layer is used for further analysis (Fig. 2).

*Noting the changes in the nearshore zone from satellite images*

Satellite images of Google Earth for the year 2011, 2013, 2014, 2015, 2017, 2018 and 2020 were used to note the periodic pattern

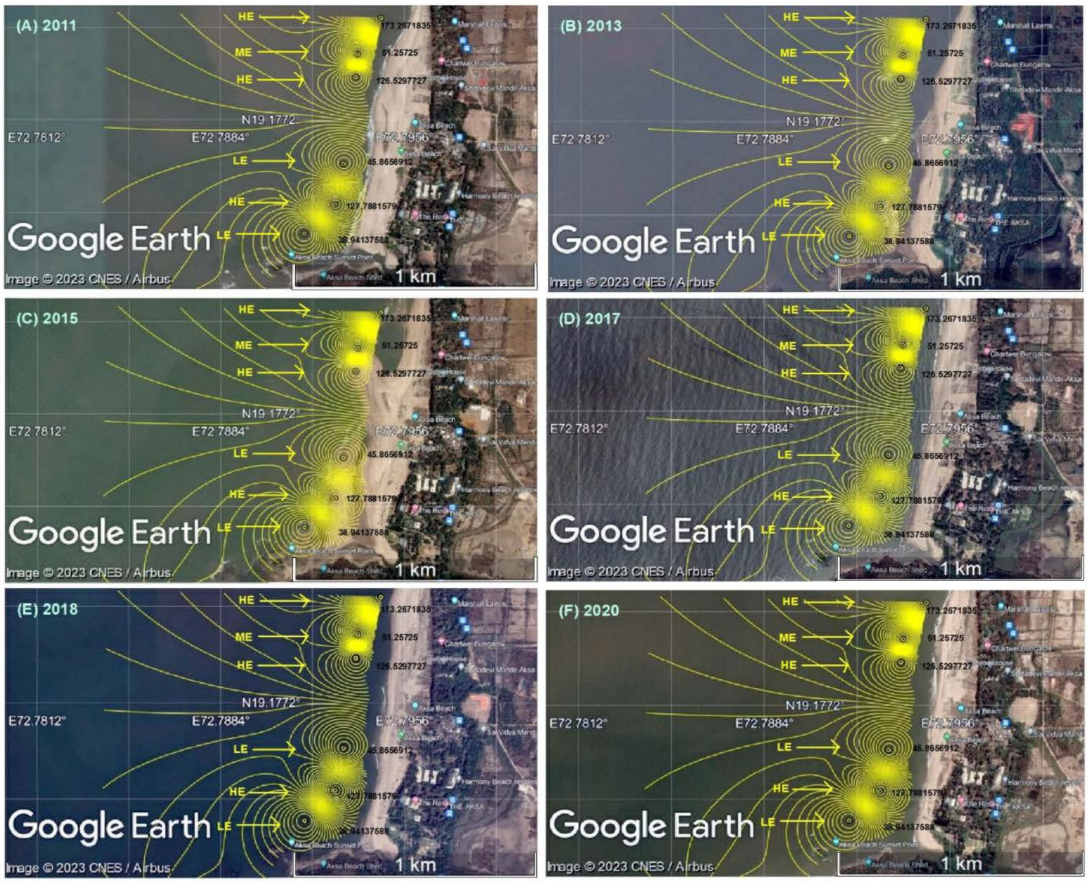


**Figure 3.** Temporal change in sediment distribution along Aksa beach (A) 2011, (B) 2013, (C) 2015, (D) 2017, (E) 2018 and (F) 2020

of formation of geomorphic features in the nearshore zone. It is challenging to see the nearshore geomorphic features on the satellite images as this zone is under water at the time of high tide. Keeping this in mind, the images of low tide conditions were chosen to show the nearshore geomorphic features. Temporal changes of the nearshore morphological signatures over a period of nearly 10 years from 2011 to 2020 were observed, focusing on the changes in the sandbars and shoals. These changes were then correlated with the wave energy patterns at the respective locations.

## Results

The overall energy pattern in the study area from Aksa beach in the north to Madh beach in the south reveals dominance of medium energy regime, interspersed by pockets of high energy and sizably large areas of low energy regimes (Fig. 2). High-energy pockets are found at the north of the study area, at the southern ends of the Aksa and Danapani beaches and in the middle of the Madh beach situated on the southern end of the studied stretch. Marked low energy regime is found along Erangal and Bhati beaches situated in the south-central part of the studied coastline.

High energy pockets are found on three beaches out of five. On the Aksa beach, three high energy pockets are found. These are at the extreme north near INS Hamla — the base of Indian navy (greater than 173 $Jm^{-2}$), opposite to Hotel Resort (greater than 126 $Jm^{-2}$) and opposite to resort (greater than 127 $Jm^{-2}$). At Danpani beach high wave energy (greater than 152 $Jm^{-2}$) is found in the middle of the beach. No high energy pockets are found on Erangal, Bhati and Madh beaches.

Medium wave energy pockets are found at Aksa beach opposite Millennium Resort (greater than 51 $Jm^{-2}$) and at Danapani beach next to shore platform (more than 88 $Jm^{-2}$), at Erangal beach next to rocky platform (around 92 J/m2). All along the Madh beach medium energy regime (90 to 96 $Jm^{-2}$) is found.

Low energy pockets are found near all the five beaches in the study area (Table 2). At Aksa beach, two low wave energy pockets are found — one in the middle part of the beach, where a depression-like feature has formed on the beach and the second one near the mouth of the tidal inlet which is situated towards the south of the Aksa beach with energies of over 45 $Jm^{-2}$ and over 38 $Jm^{-2}$

**Table 2.** Pattern of wave energy distribution over the study area

| Name of the Beach | Location ID | Wave energy ($J\ m^{-2}$) | Pattern | Name of the Beach | Location ID | Wave energy ($J\ m^{-2}$) | Pattern |
|---|---|---|---|---|---|---|---|
| Aksa | 1 | 173.27 | High | Erangal | 10 | 92.06 | Medium |
| | 2 | 51.26 | Medium | | 11 | 41.54 | Low |
| | 3 | 126.53 | High | Bhati | 12 | 22.49 | Low |
| | 4 | 45.87 | Low | | 13 | 25.47 | Low |
| | 5 | 127.79 | High | Madh | 14 | 90.01 | Medium |
| | 6 | 38.94 | Low | | 15 | 80.09 | Medium |
| Danapani | 7 | 17.73 | Low | | 16 | 91.03 | Medium |
| | 8 | 88.92 | Medium | | 17 | 96.07 | Medium |
| | 9 | 152.27 | High | | 18 | 48.56 | Low |

respectively (Fig. 3). To the immediate south of this tidal inlet and at the northern end of the Danapani beach, another pocket of low wave energy (over 17 $Jm^{-2}$) is found (Fig. 4). Further southward, from the south of the Erangal beach up to the southern end of the Bhati beach a stretch of low wave energy (values ranging from over 41 $Jm^{-2}$ to 22.49 $Jm^{-2}$) is found (Fig. 5 and 6). To its south, at the northern end of the Madh beach the stretch is interrupted by a pocket of medium energy. One pocket of low wave energy (>48 $Jm^{-2}$) is found at the extreme southern end of the Madh beach (Fig. 7).

**Nearshore features in the study area and changing patterns**

Sediment movement patterns along the beaches from Aksa to Madh are observed from satellite images. For Aksa beach, the images are observed for the years 2011, 2013, 2015, 2017, 2018 and 2020. For the remaining 4 beaches, viz. Danapani, Erangal, Bhati and Madh the changes in sediment patterns are observed for the years 2012, 2014, 2018 and 2020. Prominent changes in the sediment pattern are observed along the Aksa beach, but such changes are not seen in case of the other beaches. The location with prominent change is found near the southern end of the Aksa beach which continues up to the middle of the beach (Fig. 3A to 3F). At the southern end of the beach, a sand bar can be seen in 2013 (Fig. 3B), which was not there in 2011. The sand bar then continued to grow towards the north up to the middle of the beach, as observed in the year 2015 (Fig. 3C). It had extended in width as well as in length. In the years 2017, 2018 and 2020 (Fig. 3D, 3E and 3F), the sand bar or sand deposition was strikingly disappearing from this part. When observed in connection with the wave energy pattern in the Aksa beach area, an unique pattern of alternate high and low energy regimes could be identified within a distance of one km. Maximum sediment dynamics is associated with the areas of high wave energy, rather the intermediate pockets

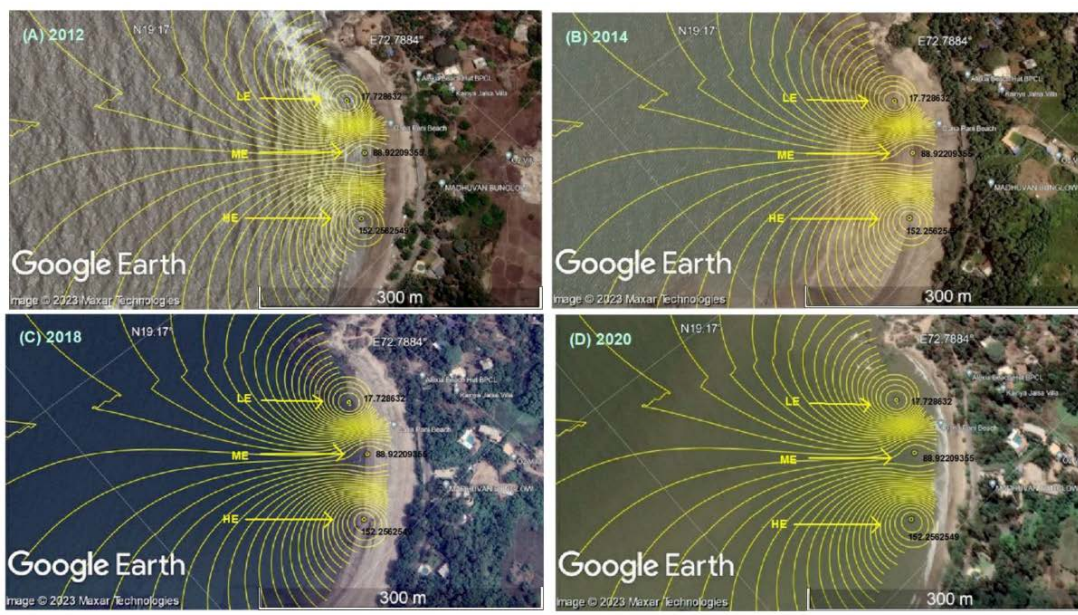


**Figure 4.** Temporal change in sediment distribution along Danapani Beach (A) 2012, (B) 2014, (C) 2018, (D) 2020.

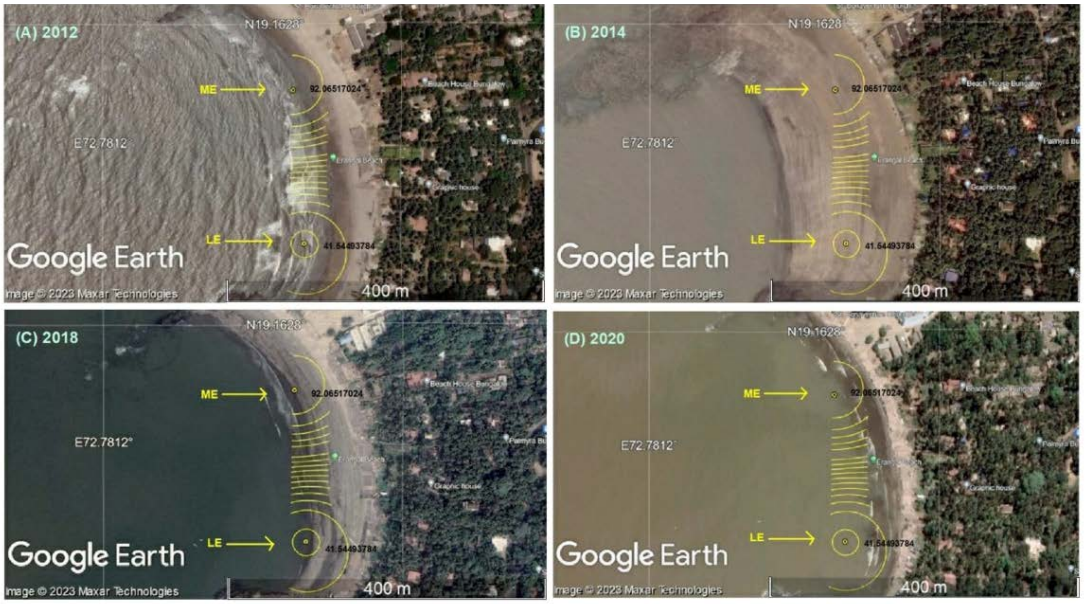


**Figure 5.** Temporal change in sediment distribution along Erangal beach (A) 2012, (B) 2014, (C) 2018, (D) 2020.

of medium and low wave energy (Fig. 3A to 3F). It is noted that such sediment dynamics has not been observed along the other beaches of Danapani, Erangal, Bhati and Madh (Fig 4, 5, 6 and 7).

## Conclusions

Analysis of wave energy reveals that there are spatial variations in wave energy in the study area, particularly along the Aksa beach. Wave data could not be collected in the areas backed by the shore platforms. The waters in front of the platforms are deep and it was very dangerous to go to the platforms to generate wave data.

Pockets of high energy are mainly found at Aksa, Danapani and Madh beaches. But mainly, the area shows medium to low energy regime. High, medium and low wave energy pockets are found alternately only at the southern end of the Aksa beach, and it is only here that major changes are found in sediment deposition pattern in the nearshore zone.

The growth of sand bars at the southern end of the Aksa beach and at the mouth of a tidal inlet are attributed to alternate pockets of high and low wave energy within a short distance of 1 km, as well as to the sediment supply by the tidal inlet. The supply of sediment for the growth of sand bar could be from three sources — sediments deposited by waves from open sea, from the beach itself and brought by tidal inlet. Out of these three, it has been observed and supported by local people that the Aksa beach very often undergoes scouring in its middle and upper part. The sediment eroded from here gets deposited near the mouth of the tidal inlet and contribute to the growth of the sand bar. Such types of or any other type of change are not found along the other four beaches over the same period. This fact needs detailed study of the area in terms of hydrodynamics and sediment dynamics along with repeated analysis of wave energy pattern. Geomorphic investigations of the beach and the offshore area are required so as to know the reasons for the differential pockets of wave energy and related sediment dynamics.

## Acknowledgements

The authors are thankful to Mr.

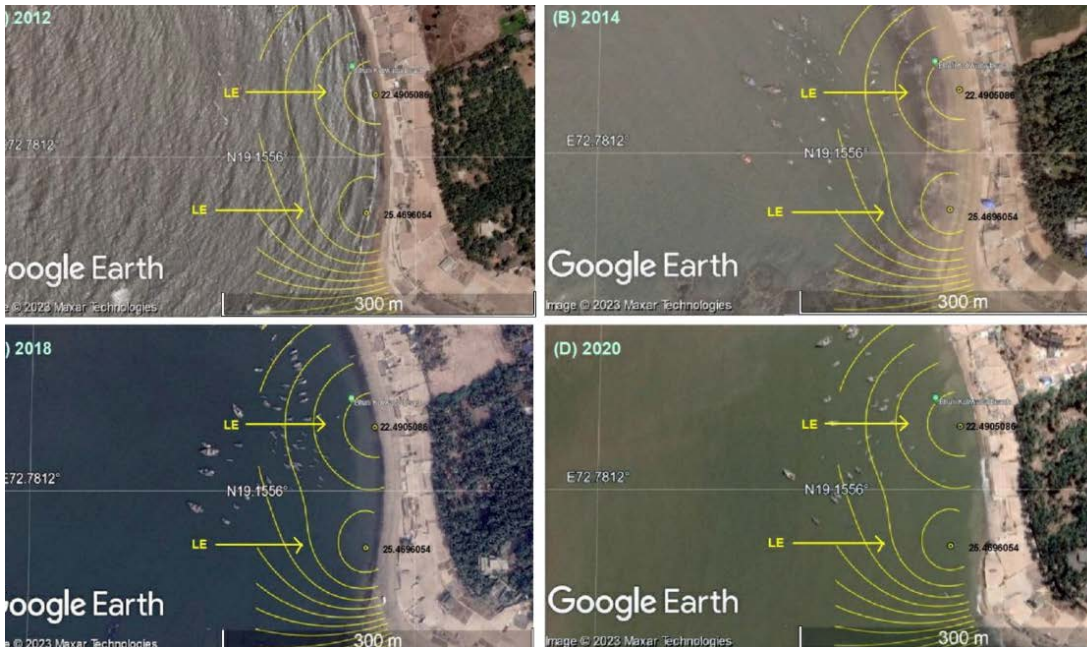


**Figure 6.** Temporal change in sediment distribution along Bhati beach (A) 2012, (B) 2014, (C) 2018, (D) 2020.

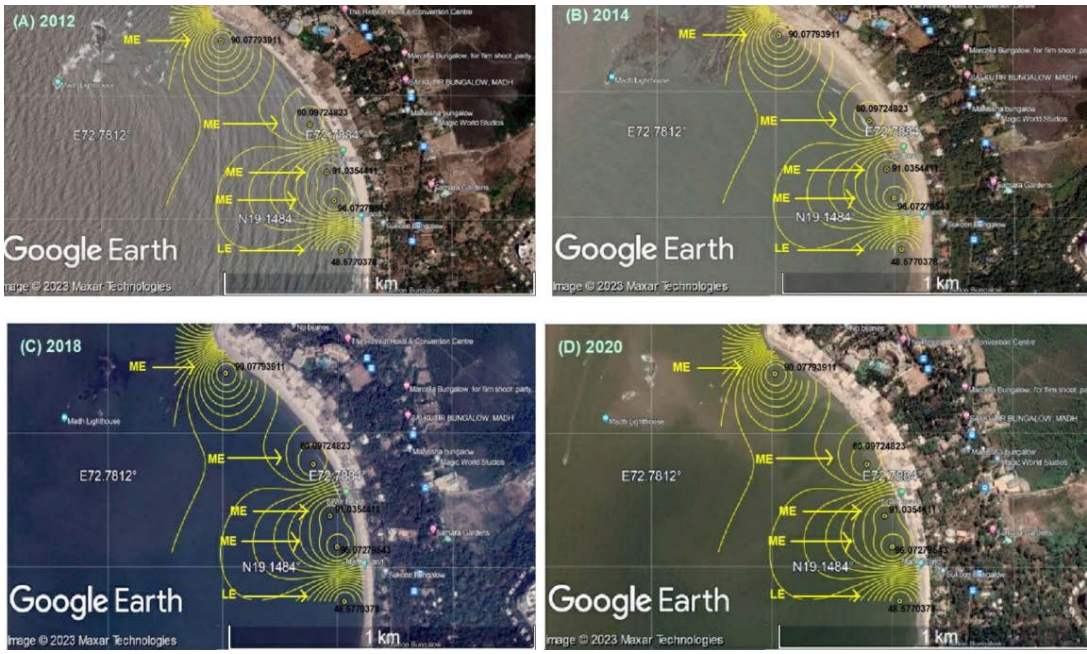


**Figure 7.** Temporal change in sediment distribution along Madh beach (A) 2012, (B) 2014, (C) 2018, (D) 2020..

Shubhankar Das, Mr. Rupjyoti, Mr.Suraj and Mr. Nathuram for helping us in the fieldwork. We are also thankful to the Head, Department of Geography, University of Mumbai for providing us necessary facilities. We are also thankful to the Chemistry Department for providing laboratory facilities during the research work. Thanks are also due to

Ms. Riddhi Kabir and Mr. Suraj Shaikh for providing cartographic assistance.

## References

Bioresita, F. and Hayati, N. (2016) Coastline change detection using Sentinel-1 satellite imagery in Surabaya, East Java, Indonesia, *Geoid,* 11(2): 190–198.

Chenthamilseivan, S., Kankara, R.S. and Rajan, B. (2014) Assessment of Shoreline Changes along Karnataka Coast, India Using GIS and Remote Sensing Techniques, *Indian Journal of Marine Sciences,* 43(7): 1–7.

Di, K., Ma, R., Wang, J. and Li, R. (2003) Coastal mapping and change detection using high-resolution IKONOS satellite imagery. In *Proceedings of the 2003 annual National Conference on Digital Government Research,* 1–4.

Dyer, K.R. (1986) *Coastal and Estuaries Sediment Dynamics.* John Wiley and Sons, London, 358p.

Kaliraj, S., Chandrasekar, N. and Magesh, N.S. (2014). Multispectral image analysis of suspended sediment concentration along the Southern coast of Kanyakumari, Tamil Nadu, India, *Journal of Coastal Sciences.* 1(1): 63–71.

Misra, A. and Balaji, R. (2015) A study on the shoreline changes and land-use/ land-cover along the South Gujarat coastline. *Procedia Engineering,* 116: 381–389. https://doi.org/10.1016/j.proeng.2015.08.311

Nassar, K., Mahmod, W.E., Fath, H., Masria, A., Nadaoka, K. and Negm, A. (2019) Shoreline change detection using DSAS technique: Case of North Sinai coast, Egypt, *Marine Georesources & Geotechnology,* 37(1): 81–95.

Rahisha, T., Goud, K.C. and Sreedhara, V. (2016) Change Detection in Mangalore Coastline Using Multi Temporal Remote Sensing Satellite Data and GIS. *International Journal of Advances in Mechanical and Civil Engineering, Special Issue,* ISSN 2394-2827: 9–14.

Sreekala, S.P., Baba, M. and Muralikrishna, M. (1998) Shoreline changes of Kerala coast using IRS data and aerial photographs, *Indian Journal of Geo-Marine Sciences,* 27(1): 144–148.

Tirkey, N., Biradar, R.S., Pikle, M. and Charatkar, S. (2005) A study on shoreline changes of Mumbai coast using remote sensing and GIS, *Journal of the Indian Society of Remote Sensing,* 33(1): 85–91. https://doi.org/10.1007/BF02989995

Vicinanza, D., Cappietti, L., Ferrante, V. and Contestabile, P. (2011) Estimation of the wave energy in the Italian offshore, *Journal of Coastal Research, Proceedings of the 11th International Coastal Symposium,* ISSN 0749-0208: 613–616.

Date received: 22 April 2023
Date accepted after revision: 31 December 2023